REVIEW ARTICLE

Intercalation of tris-(2,2′-bipyridyl) ruthenium (II) in α- and γ-zirconium phosphate: synthesis, thermal behaviour and X-ray characterization

Carla Ferragina · Romolo Di Rocco ·
Potenzo Giannoccaro · Pasquale Patrono ·
Lucantonio Petrilli

Abstract Intercalation compounds such as the ruthenium trisbipyridyl complex in inorganic layered ion-exchangers (α- and γ-zirconium phosphate) have been synthesized using the batch method. There is no loss of bipyridyl ligand from the metal ion during the exchange of the ruthenium trisbipyridyl complex in these host matrices. The materials obtained are thermally stable up to ∼330 °C (γ-phase) or ∼380 °C (α-phase). The complex decomposition occurs in one or more steps and at ∼600 °C the complex decomposition is complete. The X-ray patterns of ruthenium materials show a new phase with an increase in the interlayer distance with respect to the initial phase. Microanalysis measurements confirm the fact that the ruthenium complex is not modified when exchanged and the complex decomposition depends on its position in the host matrices.

Keywords Layered compounds · Chemical synthesis · Thermogravimetric and differential thermal analysis · X-ray diffraction

C. Ferragina (✉) · R. Di Rocco · P. Patrono
CNR-IMIP, via Salaria Km. 29.300,
00016 Monterotondo (Roma), Italy
e-mail: carla.ferragina@imip.cnr.it

P. Giannoccaro
Dipartimento di Chimica, Università di Bari,
via E. Orabona 4, 70126 Bari, Italy

L. Petrilli
CNR-ISM, via Salaria Km. 29.300,
00016 Monterotondo (Roma), Italy

Introduction

Several authors in the last decade have shown a growing interest in supporting the tris-(2,2′-bipyridyl) ruthenium (II) complex (hereafter referred to as Rubipy), compound well known for its properties as a good photosensitizer in the water-splitting system to produce hydrogen. Among the support studied many were inorganic, such as clay minerals [1–3], often dispersed as colloidal systems [4] as well as zeolites [5, 6] or semiconducting oxides [7, 8]. In all these systems the adsorption and emission spectra are similar to those in aqueous solution. In the case of compounds with ion-exchange properties such as synthetic layered α-zirconium phosphate [α-Zr(HPO$_4$)$_2$·H$_2$O, α-ZrP], in addition to the above mentioned procedure, Rubipy was added to the basic components of the ion-exchanger during the preparation either by the reflux method or direct synthesis [9, 10]. Other methods consist of exchanging Rubipy with α-ZrP-exahydrated [11]; or α-ZrP intercalated with sulphonate [12, 13]; with tetralkylammonium [14] and butilammonium derivatives [15, 16]. The latter procedure leads to less crystalline materials, even if good uptakes of the complex are achieved. Furthermore, from our experience on similar systems, there are doubts, for example, as regards the complete elimination of the tetralkylammonium or butilammonium ions during the exchange process. The presence of the complex and the co-exchanging alkylamines, during the synthesis within α-ZrP, can be avoided by the direct Rubipy ion-exchange in α-ZrP framework [12]. In this paper further studies are reported on the ion-exchange and intercalation properties of the layered inorganic acid phosphates of tetravalent metals and derived materials [17] and also the results of the investigation concerning the intercalation by ion-exchange of Rubipy in α-ZrP or sol-gel zirconium phosphate (SGZrP) or

γ-zirconium phosphate [γ-Zr(H$_2$PO$_4$)(PO$_4$)·2H$_2$O, γ-ZrP] by using the batch method and by preswelling the host matrices with ethanol. α-ZrP and SGZrP even if similar, were chosen for their different crystallinity which can influence the quantity of the ion-exchange. In fact SGZrP is less crystalline and less ordered than α-ZrP and so the ion-exchange is easier and faster. γ-ZrP was also chosen for its large cross-sectional areas which can accommodate big guests. The ion-exchange using zirconium phosphate and Rubipy, already studied in our previous paper [18], occurs by direct uptake of the Rubipy from the solution in such layered ion-exchangers. The goal of the exchange is that no loss of ligand from the complex metal ion takes place. The in situ formation method [19–22] was followed but the results obtained were no good. In this paper the study of the thermal behaviour and stability of the materials obtained and the study of their structural phases after the exchange are also reported.

Experimental

Chemicals

Ru(bipy)$_3$Cl$_2$·6H$_2$O and all other reagents were of the highest available purity and used without further purification. The compounds α-ZrP, SGZrP and γ-ZrP were prepared as reported in the references [23–25], respectively.

Materials

As the direct intercalation of the Rubipy complex into α- and sol-gel zirconium phosphate and γ-zirconium phosphate was not successful, a guest–exchange reaction was adopted and, prior to the intercalation of the complex, ethanolic forms (metastable ethanolic forms) referred to as α-ZrPEtOH [26], SGZrPEtOH [27] and γ-ZrPEtOH [28] were prepared. The weak bonds existing between ethanol and the acid sites of the different hosts ensure the eventual formation of pure phases and an increase of the initial d, interlayer distance (14.20 Å vs. 7.56 Å; 8.70 Å vs. 7.56 Å; 16.60 Å vs. 12.30 Å, respectively). The intercalation of the Rubipy species into the layered ion-exchangers was carried out following the batch procedure, at 60 °C, for a week, with Ru(bipy)$_3$Cl$_2$·6H$_2$O $1.5 \cdot 10^{-3}$ moldm^{-3} hydroalcoholic

solution (EtOH:H$_2$O = 1:1), giving α-ZrPRubipy, SGZrPRubipy and γ-ZrPRubipy materials.

Analytical measurements and instrumentation

Concentration changes of Rubipy in the supernatant before and after the contact, were determined by conventional absorption spectrophotometry, Beckman DB at $\lambda = 452$ nm, $\varepsilon = 14,600$ dm^3 mol^{-1} cm^{-1}. The XRPD patterns of the solids, at room temperature (r.t.) or higher temperatures (h.t.) were carried out in order to study the phase changes. This was done by monitoring the d and its harmonics. A Philips diffractometer (model PW 1130/00) with Ni-filtered CuK$_\alpha$ radiation ($\lambda = 1.541$ Å) was used. The thermal behaviour, organic ligand and water content of the solids of the intercalation compounds were determined with a simultaneous TG-DTA Stanton Redcroft 1500 thermoanalyzer, Pt crucibles, heating rate 10 °C min^{-1}, heated up to 1,100 °C to constant weight in an air or nitrogen flow. The content of the ligand bipy (carbon, nitrogen) in the materials was also determined using a Fisions 1108 elemental microanalyser (M.A.).

Results

Synthesis

The uptake of Rubipy using the ethanolic form of the three examined exchangers occurs via H$^+$/[Ru(bipy)$_3^{2+}$] ion-exchange, since the pH of the supernatant decreases to a value, upon completion, that depends on the initial exchanger itself. In Table 1 the chemical formula of all the ruthenium materials obtained with their d and colour are reported. The α-ZrPRubipy material was prepared by contacting 1 mmol of α-ZrPEtOH with a quantity of Ru(bipy)$_3$Cl$_2$·6H$_2$O $1.5 \cdot 10^{-3}$ moldm^{-3} hydroalcoholic solution, at 60 °C, for 4 days, so that a maximum loading of 0.5 moles of Rubipy/mole of exchanger could be eventually achieved. As soon as the exchange occured the material colour changed from white to brilliant orange. The pH of the supernatant decreased from ~ 6.10 (initial value of Rubipy solution) to a value of ~ 4.18. The solid was filtered off and the change in the concentration of the Rubipy solution before and after the contact was determined. The highest cation uptake was obtained with

Table 1 Obtained compounds and some of their physico-chemical characteristics

Chemical formula	d (Å)	Colour
α-ZrH$_{1.74}$[Ru(bipy)$_3$]$_{0.13}$(PO$_4$)$_2$·2.70H$_2$O	14.24	Brilliant orange
SGZrH$_{1.97}$[Ru(bipy)$_3$]$_{0.025}$(PO$_4$)$_2$·2.45H$_2$O	7.60 + 14.24	Pale orange
(γ-ZrH$_{1.60}$[Ru(bipy)$_3$]$_{0.20}$(PO$_4$)$_2$·3.20H$_2$O	18.40	Brilliant orange

0.13 moles of Rubipy/mole of exchanger. The kinetic uptake was also carried out in batches at set time intervals. The uptake of ∼50% of the total amount exchanged of the complex solution used, was achieved after ∼5 h, and 100% after 4 days. This can be explained by the steric hindrance (Ru^{2+} surrounded by 6 rings) of the complex inserted. Attempts were made to obtain higher uptakes of the complex by: (i) increasing the concentration of the contact solution; (ii) doubling the volume of the contact solution; (iii) increasing the number of days of contact; (iv) using the propanolic form of the exchanger which has higher values of d compared with those of ethanolic forms (15.60 Å vs. 14.20 Å, respectively). However, the results obtained were poor and not satisfying (Table 2). As far as the material obtained from the SGZrPEtOH is concerned the highest Rubipy uptake was obtained with 0.025 moles of Rubipy/mole of exchanger. (It must be remembered that α-ZrP directly contacted with EtOH and subsequently with the Rubipy solution does not give any exchange because α-ZrP does not intercalate the EtOH, as reported in [23]). As regards SGZrP it is less crystalline and less ordered than α-ZrP and so the exchange could be easier, but in this case neither a hydrothermal synthesis (HB) nor prolonged time of batch contact (Table 3) [29] enhances the complex exchange which results less than in the case of α-ZrP. The ion-exchange is improved only by using a more diluted solution ($7 \cdot 10^{-4}$ moldm^{-3} vs. $1.5 \cdot 10^{-3}$ moldm^{-3}). In the case of γ-ZrP the Rubipy materials were synthesized as had been previously done in the case of α-materials. The pH value decreased (initial pH = 6.10 vs. final pH = 3.12) giving a final loading of 0.20 moles of Rubipy/mole of exchanger. As regards the kinetic uptake, performed at different set time intervals by γ-ZrPEtOH and the Rubipy solution, 60% of the maximum uptake of the ruthenium complex was achieved after 1 h; 80% after 24 h; 100% after 4 days. Rubipy uptakes were higher than in the case

of α-ZrP or SGZrP (Table 4), but there was never a 100% of ion-exchange or more than 20%, because of the steric hindrance of the Rubipy complex.

Thermal behaviour

In Fig. 1 the TG-DTA curves of ruthenium derivatives of α-ZrP, SGZrP and γ-ZrP are compared with the initial materials. It is clearly evident that, in the case of the α-derivative, after the dehydration process which occurs between 25 and 350 °C, the decomposition of the Rubipy complex begins and is complete at ∼620 °C. The Rubipy decomposition occurs in two well defined steps, evident both from the TG and the DTA curves. The decomposition occurs with a different kinetic: the first loss is rapid and the second one more gradual. Immediately after the first loss the second loss starts and in the TG curve it can be observed as an inflection. In correspondence with the DTA curve, intense sharp and broad exothermic peaks at 450 °C and at 490 °C occur, respectively. The colour of the material is dark orange at 430 °C and turns to grey at ∼480–500 °C, when the complex has finished decomposing. In the range of temperature between 450 and 620 °C, the total weight loss comprises the concomitant water elimination arising from the condensation of the unchanged acid phosphate groups to give zirconium pyrophosphate. A small exothermic peak at 990 °C is due to the formation of cubic zirconium pyrophosphate. In the case of SGZrPRubipy the thermal behaviour is similar to that of α-ZrPRubipy: immediately after dehydration between 25 and 350 °C, two subsequent weight losses occur up to ∼620 °C. From the DTA curve the first loss at 430 °C (a sharp exothermic peak as in the α-case) is related with the complex decomposition. The second one at 550 °C (endothermic peak) is related to the water arising from the condensation of the phosphate groups of the

Table 2 C% and N% of the bipyridyl at the appropriate temperature[a]

Materials	%C 200 °C	%N	%C 380 °C	%N	%C 430 °C	%N
Ru(bipy)$_3$Cl$_2$·6H$_2$O	55.04…	…12.91	54.21…	…12.66	2.32	1.06
	29.38C	**5.90 N**	**28.91C**	**5.78 N**	**1.23C**	**0.48 N**
					Grey	
(α-ZrPRubipy 5 h	7.58	1.64	7.31	1.64	5.39	1.31
	0.20	**0.20**	**0.19**	**0.20**	**0.14**	**0.16**
					Dark orange	
α-ZrPRubipy 2 days	12.63	2.90	12.62	2.87	6.27	1.71
	0.37	**0.36**	**0.37**	**0.36**	**0.18**	**0.21**
					Dark orange	
α-ZrPRubipy 4 days	13.40	3.09	13.00	2.91	7.03	1.96
	0.39	**0.39**	**0.39**	**0.38**	**0.204**	**0.24**
					Dark orange	

[a] Bold numbers are diamines content at established temperatures

Table 3 C% and N% of the bipyridyl at the appropriate temperature[a]

Materials	%C 200 °C	%N	%C 380 °C	%N	%C 430 °C	%N
SGRubipy (not preswelled)	1.21	0.24	1.19	0.23	abs	abs
	0.030	**0.024**	**0.030**	**0.024**	Light grey	
SGRubipy $7 \cdot 10^{-4}$moldm^{-3}	3.17	0.68	3.11	0.62	0.25	ass
	0.075	**0.072**	**0.069**	**0.069**	Light grey	
SGRubipy $1.5 \cdot 10^{-3}$moldm^{-3}	1.51	0.29	1.50	0.28	0.12	abs
	0.036	**0.030**	**0.036**	**0.030**	Light grey	
SGRubipy (more days of batch contact)	3.15	0.65	3.12	0.62	0.22	abs
	0.072	**0.072**	**0.069**	**0.069**	Light grey	
SGRubipy HB	1.56	0.31	1.50	0.27	0.08	abs
	0.038	**0.032**	**0.037**	**0.031**	Light grey	

[a] Bold numbers are diamines content at established temperatures

Table 4 C% and N% of the bipyridyl at the appropriate temperature[a]

| Materials	%C 200 °C	%N	%C 380 °C	%N	%C 430 °C	%N
(γ-ZrPRubipy 5 h	12.39	2.71	9.62	2.49	1.81	0.93
	0.36	**0.33**	**0.27**	**0.30**	**0.027**	**0.099**
					Dark orange	
γ-ZrPRubipy 2 days	14.03	3.11	10.38	2.72	1.95	1.01
	0.42	**0.39**	**0.29**	**0.33**	**0.030**	**0.108**
					Dark orange	
γ-ZrPRubipy 4 days	20.61	4.90	14.86	4.37	2.79	1.62
	0.60	**0.63**	**0.42**	**0.54**	**0.045**	**0.174**
					Dark orange	

[a] Bold numbers are diamines content at established temperatures

unchanged acid phosphate groups to give zirconium pyrophosphate. This fact is confirmed by the microanalysis data (Table 3). This is because the amount of the Rubipy complex intercalated is very small. The colour of the material is light grey at 430 °C, when the ruthenium complex has finished decomposing. This confirms the fact that few H$^+$ of the POH groups on the surface have been exchanged and they are so weakly linked to the matrix. An evident exothermic peak at 1,000 °C, sharper than that observed in α-ZrPRubipy, is due to the cubic zirconium pyrophosphate formation. As regards γ-ZrPRubipy, after dehydration between 25 and 330 °C, losses suddenly occur, in three steps, up to ~600 °C with different kinetics and three exothermic peaks are evident in the DTA curve, at 400, 440 and 510 °C. The third loss also comprises both the ruthenium complex decomposition and the water arising from the phosphate condensation to give pyrophosphate groups. At 950 °C a small exothermic peak of cubic zirconium pyrophosphate formation is present. The way the Rubipy complex decomposes differs in these three host matrices and this is due to its different position after the ion-exchange. In fact the Rubipy exchange occurs first of all externally and decomposes more easily (less strongly

linked to the host matrix). This is the case of SGZrPRubipy whose complex decomposition occurs in only one step. In the case of α-ZrPRubipy and γ-ZrPRubipy the ion-exchange occurs inside the layers of the exchanger (more strongly linked to the host matrices). The thermal behaviour of Ru(bipy)$_3$Cl$_2 \cdot 6H_2O$, as a pure salt, not intercalated, was also performed. The TG-DTA curves show dehydration between 25 and 320 °C, and the complex decomposition between 330 and 520 °C (Fig. 2). α-ZrPRubipy, SGZrPRubipy and γ-ZrPRubipy materials also underwent thermal treatment, in a nitrogen flow, in the TG-DTA simultaneous apparatus. As can be observed in Fig. 3, α- and γ-ZrPRubipy behave similarly: in the DTA curves the exothermic peaks, related to the complex decomposition, are absent whereas continuous and very slow complex loss is evident in the TG curves, between 330 and 680 °C (α-phase) and between 330 and 880 °C (γ-phase). In the case of SGRubipy the loss between 400 and 600 °C is continuous but rapid with a sharp endothermic peak related to the water arising from the condensation of phosphate groups to give zirconium pyrophosphate. This process, is more evident than in the case performed in an air flow.

XRPD

As reported in Figs. 4–6 the diffractograms of the materials obtained are still layered and the d increase is due to the well ordered complex intercalation between the layers. Just after one day of batch contact, the diffractogram of the α-ZrPRubipy material obtained shows some changes with respect to the initial material. The d at 14.60 Å shows an increase of ~7 Å with respect to the initial material (α-ZrP $d = 7.60$ Å). This new phase corresponds to an intercalation of the complex into α-ZrP with well defined peaks in the XRPD and are indicative of a well defined crystalline structure. The complex is bonded to the phosphate groups not on the same plane, but between two planes. The d and the free height [30] of 8.30 Å (14.60–6.30 Å, layer
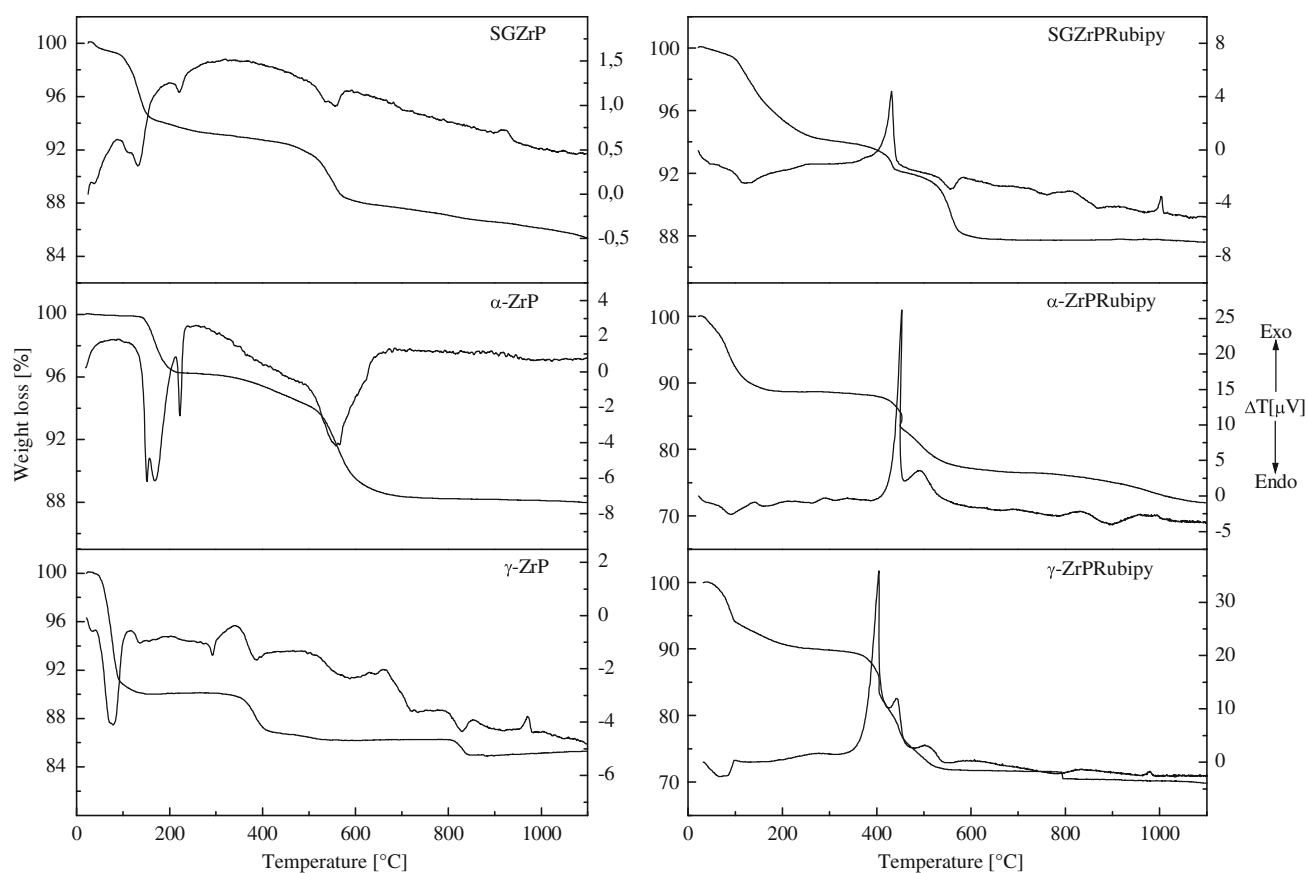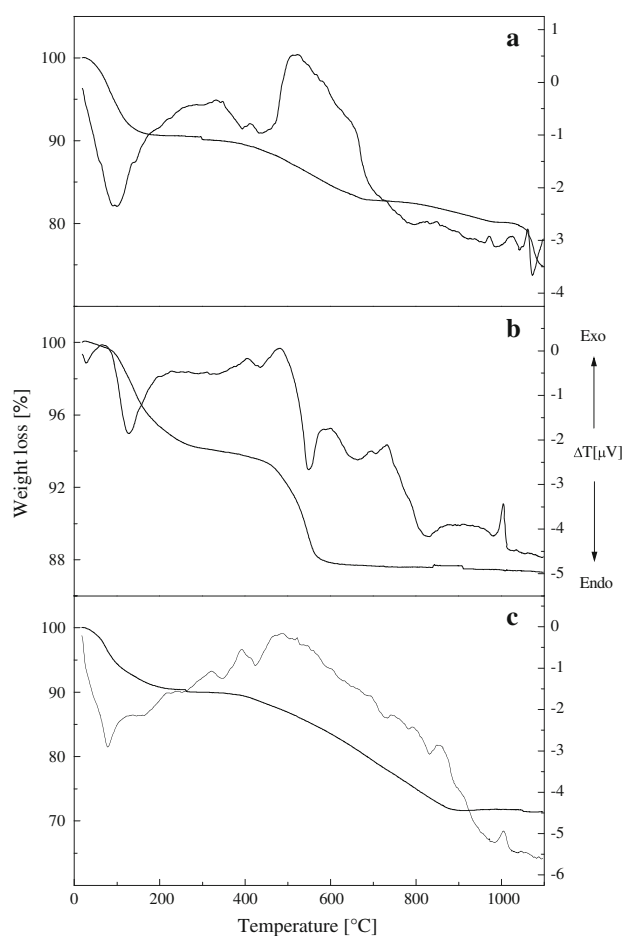
Fig. 1 TG-DTA curves of the obtained α-ZrPRubipy, SGZrPRubipy and γ-ZrPRubipy materials in comparison with their precursors
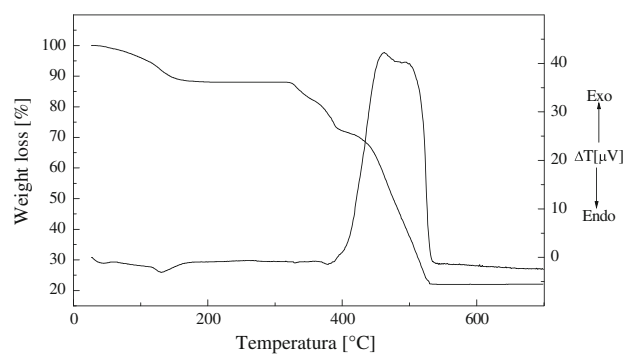
Fig. 2 TG-DTA curves of the pure salt Ru(bipy)$_3$Cl$_2$·6H$_2$O

thickness) are indicative of the formation of an intercalated monolayer and are in accordance with the complex arrangement between the layers of the ion-exchanger (Fig. 4a). The disappearance of the diffraction lines of α-ZrP, depending on the quantity of Rubipy exchanged, suggests that every layer of the material contains guest molecules and only one phase is present after the exchange. This is the case of α-ZrPRubipy containing ≥ 0.13 moles of Rubipy/mole exchanger and this could explain why the quantity of the cation exchange is not so big. In the case of α-ZrPRubipy containing <0.13 moles because of such low

loadings, the X-ray patterns show the co-presence of α-ZrP (7.60 Å) and the new layered phase (14.60 Å) (Fig. 4b). The former phase decreases as the uptake proceeds. As regards the SGZrPRubipy the small uptake of the complex gives an X-ray diffractogram similar to that of the initial SGZrP: the ion-exchange of the complex is only external. In the case of γ-ZrPRubipy the d at 18.52 Å shows an increase of ∼6.20 Å with respect to the initial material (γ-ZrP = 12.30 Å) and the free height obtained, 9.32 Å (18.52–9.20 Å, layer thickness) is in accordance with the complex lodging in the exchanger. The thermal stability of all these materials is also confirmed by the X-ray measurements performed at h.t. In Figs. 5, 6 (α-ZrPRubipy and γ-ZrPRubipy, respectively, are recorded at various temperatures) it is evident that as far as α-ZrPRubipy is concerned the layered structure is maintained up to ∼500 °C: at this temperature the d and its harmonic are still present, but their intensity has decreased; subsequent reflections are quite amorphous up to ∼950 °C; at 1,100 °C (grey material) the material shows only cubic zirconium pyrophosphate reflections. At 1,350 °C (white colour) cubic zirconium pyrophosphate and two reflections (2θ = 28.15*–35.20*, Fig. 5) related to ruthenium oxide RuO$_2$ are present [31]. In the case of γ-ZrPRubipy the d

Fig. 3 TG-DTA curves of (**a**) α-ZrPRubipy, (**b**) SGZrPRubipy and (**c**) γ-ZrPRubipy, performed in nitrogen flow

Fig. 4 XRPD of α-ZrPRubipy: (**a**) with Rubipy = 0.13 moles/mole of exchanger; (**b**) with Rubipy ≤0.13 moles/mole of exchanger. (**c**) α-ZrP, for comparison

decrease is noticeable, with respect to the initial material, up to 500 °C: 18.52 Å (r.t)–17.26 Å (300 °C)–9.94 Å (500 °C). The amorphization occurs up to ∼900 °C. At 950 °C cubic zirconium pyrophosphate and two reflections ($2\theta = 28.15^*$–35.20^*, Fig. 6) related to the ruthenium oxide RuO_2 are present. At 1,350 °C the diffractogram is equal to that of α-ZrPRubipy at the same temperature. This is in accordance with the thermal behaviour of the ruthenium materials: as previously observed the TG curve of the γ-material shows the exothermic peak of pyrophosphate formation at ∼950 °C, whereas at this temperature the reaction is almost absent in the case of α-ruthenium material
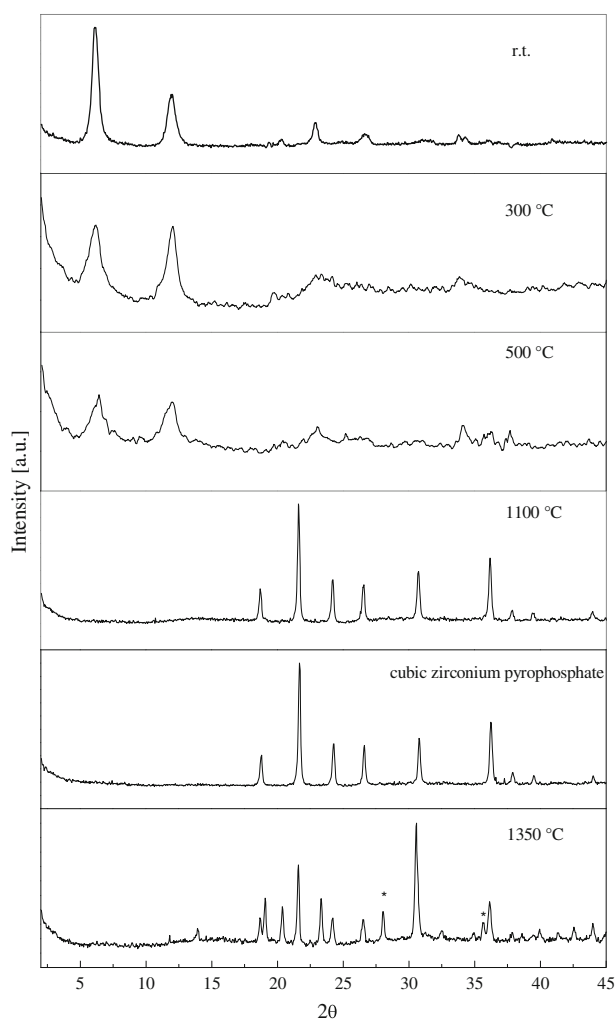
Microanalysis measurements

In Tables 2–4 a comparison of the microanalysis data (of the ruthenium materials and of the $Ru(bipy)_3Cl_2·6H_2O$) obtained at various temperatures is reported. As regards $Ru(bipy)_3Cl_2·6H_2O$ (Table 2) C% and N% values at 200 °C and 380 °C are approximately the same as the

theoretical data related to anhydrous salt. In the case of α-ZrPRubipy materials, the measurements performed at 200 °C (dehydrated materials), 380 °C (when the complex decomposition starts) and 430 °C (when the complex decomposition is almost complete) show that at 380 °C the values are similar to those obtained at 200 °C indicating that the materials are thermally stable up to ∼380 °C and the colour is still brilliant orange. At 200 and 380 °C the C% and N% demonstrate that the organic ligand is in a molar ratio with ruthenium, Ru:ligand = 1:3, thus indicating that the tris-chelate complex species maintain their full integrity and enter in the exchanger and remain unchanged as previously observed (e.g. in Table 2: theoretical data of the ratio C/N in the case of anhydrous $Ru(bipy)_3Cl_2$ is 4.28; in the case of α-ZrPRubipy 4 days, is 4.33). At 430 °C the C% and N% indicate that the loss is on average ∼48% of all C present and ∼39% of all N present. Consequently it can be deduced that the Rubipy complex is linked to the host matrix through N and this
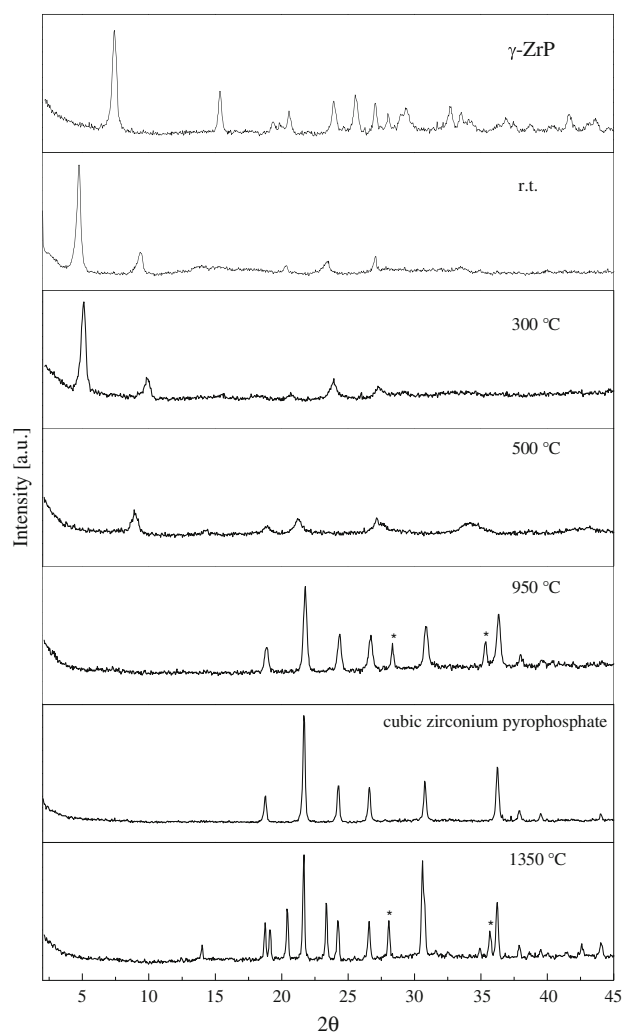
Fig. 5 XRPD of α-ZrPRubipy recorded at various temperatures

Fig. 6 XRPD of γ-ZrPRubipy recorded at various temperatures and γ-ZrP for comparison

bond is stronger than C. As far as SGRubipy is concerned results, related to the complex exchanged, are better when the solution is diluted ($\sim 10^{-4}$ moldm^{-3}); at 430 °C there is no residual C% and N%; the colour is light grey because the number of particles of the complex that are decomposed are a few. In the case of γ-ZrPRubipy (Table 4) the data are in accordance with those observed from TG-DTA curves. Contrary to the α-derivative, at 380 °C and at 430 °C different values of C% and N% can be observed related to ligand combustion. The losses are on average $\sim 30\%$ of all C present and $\sim 14\%$ of all N present; at 430 °C they are $\sim 92\%$ of all C present and $\sim 72\%$ of all N present.

Conclusions

From the results presented it can be deduced that stable Rubipy complex can be intercalated in inorganic ion-exchanger matrices possessing a nonrigid structure such as

α- and SG zirconium phosphates and γ-zirconium phosphate. The incorporation of nonhomogeneous Rubipy during the synthesis is avoided by the direct ion-exchange of Ruby in these matrices.

The exchange is more successful in the case of γ-ZrP > α-ZrP > SGZrP depending on the interlayer distance of the host matrices. In the case of α-ZrPRubipy a pure monolayer phase is obtained with the maximum uptake being 13% of the ion-exchange capacity of the exchanger and showing a good degree of crystallinity. Its thermal behaviour indicates a stability up to ~ 380 °C when the decomposition complex begins. In the case of SGZrPRubipy the few cation exchanged do not change the XRPD diffractogram while the TG-DTA curves indicate the decomposition of the Rubipy complex in only one step. As far as γ-ZrPRubipy is concerned the bigger complex exchange, 20% of the ion-exchange capacity, is due to the bigger d with respect to the previous exchangers and a pure

monolayer phase is obtained. Its thermal behaviour demonstrates the complex decomposition in more steps, the first one starting at temperature lower than in the case of α-materials. The different steps of complex decomposition of the three host matrices is indicative of the different position of the complex (whether inside or outside the framework) of the ion-exchangers. Microanalysis values obtained from the ruthenium materials at various temperatures indicate that the Rubipy is not modified when exchanged and 3 bipy are still present in the exchanged materials. At 430 °C the different C% and N% data confirm that the Rubipy complex is linked to the host matrices by means of N and this bond is stronger than that of C.

References

1. Della Guardia, R.A., Thomas, J.K.: Photoprocesses on colloidal clay systems. Tris(2, 2′-bipyridinium)ruthenium(II) bound to colloidal kaolin and montmorillonite. J. Phys. Chem. **87**, 990–998 (1983). doi:10.1021/j100229a016
2. Schoonheydt, R.A., De Pauw, P., Vliers, D., De Schrijver, F.C.: Luminescence of tris(2,2′-bipyridine)ruthenium(II) in aqueous clay mineral suspensions. J. Phys. Chem. **88**, 5113–5118 (1984). doi:10.1021/j150665a062
3. Joshi, V., Kothar, D., Ghost, K.: On the interaction of poly(pyridine)ruthenium(II) optical antipodes intercalated in montmorillonite clay. J. Am. Chem. Soc. **108**, 4650–4658 (1986). doi:10.1021/ja00275a066
4. Memming, R.: Photoelectrochemical utilization of solar energy, in "Photochemistry and Photophysics", vol. II, p. 143. CRC Press, Boca Raton, FL (1990)
5. De Wilde, W., Peeters, G., Lunsford, J.H.: Synthesis and spectroscopic properties of tris(2,2′-bipyridine)ruthenium(II) in zeolite Y. J. Phys. Chem. **84**, 2306–2310 (1980). doi:10.1021/j100455a019
6. Quayle, W.H., Lunsford, J.H.: Tris(2,2′-bipyridine)ruthenium(III) in zeolite Y: characterization and reduction on exposure to water. Inorg. Chem. **21**, 97–103 (1982). doi:10.1021/ic00131a019
7. Willner, I., Yang, J.M., Laane, C., Otvos, J.W., Calvin, M., Memming, R.: Electron transfer reaction of excited ruthenium (II) complexes at semiconductor electrodes. Surf. Sci. **101**, 551–558 (1980). doi:10.1016/0039-6028(80)90649-4
8. Perry, J.W., McQuillon, A.J., Anson, F.C., Zewall, A.H.: Laser spectroelectrochemistry of a ruthenium(II) tris(bipyridyl) derivative adsorbed on graphite electrodes. J. Phys. Chem. **87**, 1480–1489 (1983)
9. Yates, R.C., Kuznicki, S.M., Lloyd, L.B., Eyring, E.M.: Tris (2,2′-bipyridine) ruthenium (II) electron-transfer in a layered zirconium phosphate. J. Inorg. Nucl. Chem. **43**, 2355–2358 (1981). doi:10.1016/0022-1902(81)80264-3
10. Vliers, D.P., Schoonheydt, R.A.: Synthesis and luminescence of ruthenium tris(2,2′-bipyridine)–zirconium phosphates. J. Chem. Soc., Faraday Trans. **81**, 2009–2015 (1985). doi:10.1039/f19858102009
11. Marti, A.A., Colon, J.L.: Direct ion exchange of tris(2,2′-bipyridine)ruthenium(II) into an α-zirconium phosphate framework. Inorg. Chem. **42**(9), 2830–2837 (2003). doi:10.1021/ic025548g
12. Colon, J.L., Yang, C.Y., Clearfield, A., Martin, C.R.: Optical investigation of the chemical microenvironment within the layered solid zirconium phosphate sulphophenylphosphonate. J. Phys. Chem. **92**, 5777–5781 (1988). doi:10.1021/j100331a046
13. Colon, J.L., Yang, C.Y., Clearfield, A., Martin, C.R.: Photophysic and photochemistry of tris(2,2′-bipyridyl)ruthenium (II) within the layered inorganic solid zirconium phosphate sulphophenylphosphonate. J. Phys. Chem. **84**, 874–881 (1990). doi:10.1021/j100365a068
14. Vliers, D.P., Collin, D., Schoonheydt, R.A., De Schrijver, F.C.: Synthesis and characterization of aqueous tris(2,2′-bipyridine) ruthenium(II)-zirconium phosphate suspension. Langmuir **2**, 165–169 (1986). doi:10.1021/la00068a009
15. Shi, S., Zhou, J., Zong, R., Ye, J.: Spectroscopic studies of tris(2,2′-bipyridine)ruthenium(II) intercalated to modified α-zirconium phosphate. J. Lumin. **122–123**, 218–225 (2007). doi:10.1016/j.jlumin.2006.01.095
16. Kumar, C.V., Williams, Z.J.: Supramolecular assemblies of tris(2,2′-bipyridine)ruthenium(II) bound to hydrophobically modified alpha-zirconium phosphate: photophysical studies. J. Phys. Chem. **99**, 17632–17639 (1995). doi:10.1021/j100049a025
17. Ferragina, C., Frezza, A., La Ginestra, A., Massucci, M.A., Patrono, P.: Intercalation properties of layered metal(IV) phosphates towards organic bases, metal complexes and metal oxides, In: Occelli, M.L., Robson, H., (eds.) "Expanded Clays and other Microporous Solids", vol. II, chapt. 13, N.Y., p. 263, (1992)
18. Ferragina, C., La Ginestra, A., Massucci, M.A., Patrono, P., Cafarelli, P.: Intercalation of Ru(II) aromatic diamine complexes in α-and γ-zirconium and titanium phosphates, Proceedings of the International Conference ION-EX'93, In: Dyer, A., Hudson, M.J., Williams, P.A., (eds.) Wrexham (UK), p. 345 (1993)
19. Ferragina, C., La Ginestra, A., Massucci, M.A., Patrono, P., Tomlinson, A.A.G.: Intercalation of 2,2′-bipyridyl into α-zirconium phosphate and in-situ formation of Co^{2+}, Ni^{2+} and Cu^{2+}-2,2′-bipyridyl complex pillars. J. Phys. Chem. **89**, 4762–4769 (1985). doi:10.1021/j100268a022
20. Ferragina, C., La Ginestra, A., Massucci, M.A., Patrono, P., Tomlinson, A.A.G.: Pillaring of layers in α-zirconium phosphate by 1,10-phenanthroline and bis-(1,10-phenanthroline) copper(II): formation of complex pillars in-situ. J. Chem. Soc., Dalton Trans. 265–271 (1986) doi:10.1039/dt9860000265
21. Ferragina, C., La Ginestra, A., Massucci, M.A., Patrono, P., Tomlinson, A.A.G.: Coordination of Co^{2+}, Ni^{2+} and Cu^{2+} to 2,9-dimethyl–1,10-phenanthroline intercalated in α-zirconium phosphate: evidence for dimmers. Mater. Res. Bull. **22**, 29–36 (1987). doi:10.1016/0025-5408(87)90146-2
22. Ferragina, C., Massucci, M.A., Tomlinson, A.A.G.: Pillar chemistry. Part 5. Intercalation of 2,2′-bipyridyl, 1,10-phenanthroline and 2,9-dimethyl-1,10-phenanthroline into γ-zirconium phosphate and formation of interlayer copper (II) complexes. J. Chem. Soc., Dalton Trans. 1191–1196 (1990) doi:10.1039/dt9900001191
23. Alberti, G., Torracca, E.: Crystalline insoluble salts of polybasic metals—II. Synthesis of crystalline zirconium or titanium phosphate by direct precipitation. J. Inorg. Nucl. Chem. **30**, 317–318 (1968). doi:10.1016/0022-1902(68)80096-X
24. Livage, J., Barboux, P., Benhamza, H., Bouhaouss, A., Josien, F.A.: Sol-gel synthesis of Zr(HPO$_4$)$_2$·H$_2$O. J. Mater. Chem. **1**(4), 681–687 (1991). doi:10.1039/jm9910100681
25. Yamanaka, S., Tanaka, M.: Formation region and structural model of γ-zirconium phosphate. J. Inorg. Nucl. Chem. **41**, 45–48 (1979). doi:10.1016/0022-1902(79)80391-7
26. Costantino, U.: Intercalation of alkanols and glycols into zirconium(IV) hydrogenphosphate monohydrate. J. Chem. Soc., Dalton Trans. 402–405 (1979) doi:10.1039/dt9790000402
27. Ferragina, C., Cafarelli, P., De Stefanis, A., Di Rocco, R., Petrilli, L.: Synthesis and characterization of sol-gel zirconium phosphate with template surfactants by different methods. J. Therm. Anal. Calorim. **71**, 1023–1033 (2003). doi:10.1023/A:1023311201187

28. Costantino, U.: Intercalation of alkanols and alkylamines in insoluble acid salts of tetravalent metals having a layered structure of γ-type. J. Inorg. Nucl. Chem. **43**, 1985–1990 (1981). doi:10.1016/0022-1902(81)80404-6

29. Ferragina, C., Di Rocco, R.: Compounds of γ-zirconium hydrogen phosphate with cadmium ions. Part 1. Preparation, thermal behavior and X-ray characterization of the Cd^{2+} exchanged and CdS intercalated materials. Mater. Res. Bull. **43**, 1981–1989 (1999). doi:10.1016/S0025-5408(99)00221-4

30. Maireles-Torres, P., Olivera-Pastor, P., Rodriguez-Castellon, E., Jmenez-Lopez, A., Tomlinson, A.A.G.: Porous chromia-pillared α-zirconium phosphate materials prepared *via* colloid methods. J. Mater. Chem. **1**(5), 739–743 (1991). doi:10.1039/jm9910100739

31. Powder Diffraction File, International Centre For Diffraction Data, Sets 1–43, 573 (1993)